IEEE Robotics and Automation Letters (RA-L) paper, presented at ICRA 2026, Vienna, Austria. Cite as RA-L paper.

Estimation of Gait Phase of Human Stair Descent Walking Based on Phase Variable Approach

Myeongju Cha, *Graduate Student Member, IEEE*, and Pilwon Hur, *Member, IEEE*

***Abstract*—Synchronization between a wearer and a lower limb powered prosthesis is important for effective control. Typically, phase variable-based phase estimation methods are employed. However, there is a noticeable lack of studies focusing on estimating the gait phase during stair descent, likely due to the difficulty in generating a reliable phase variable. In most studies, the thigh angle is used to generate phase variables for level walking because it follows a sinusoidal pattern. However, during stair descent, the thigh angle exhibits only a partially sinusoidal shape, making it challenging to apply the methods used for level walking. In this study, we propose a novel phase variable generation method to address the difficulty of using only the thigh angle for stair descent. To estimate the gait phase reliably, the phase variable is defined differently for the stance and swing phases: the hip position is used to generate the phase variable during the stance phase, and the thigh angle is used during the swing phase. These phase variables are then unified into a single phase variable (PV-ENT) for the entire gait cycle of stair descent. During this unification process, a non-smooth transition occurs around the phase transition point. To address this, a blending method is applied. The proposed method was validated using the data from 12 healthy subjects, collected through a motion capture system and IMU sensors. The results demonstrate a reliable phase estimation performance. Moreover, the blending method successfully improves the smoothness of the phase variable around the phase transition point without reducing the overall phase estimation performance.**

***Index Terms*—Wearable robotics, prosthetics and exoskeletons, intention recognition, gait phase estimation, stair descent.**

I. Introduction

SYNCHRONIZATION between a wearer and a powered lower limb prosthesis allows the prosthesis to generate appropriate behavior, providing a comfortable gait for the wearer [1], [2], [3], [4], [5], [6], [7], [8]. If the prosthesis is not synchronized with the wearer, it can produce undesirable behavior, potentially resulting in falls or injuries. Over the years, studies have been conducted to synchronize the prosthesis with the wearer in various walking environments. Myoelectric and dynamic information have both been used as methods for achieving synchronization. Myoelectric information offers the advantage of providing more direct insights into the wearer's intention, which can enhance the responsiveness of the prosthesis [9], [10], [11], [12], [13], [14], [15], [16]. However, myoelectric signals can be affected by factors such as sensor placement or skin conditions, leading to variability. On the other hand, dynamic information is more stable, as it relies less on direct sensor interaction with the wearer [17]. Due to its reliability, dynamic information is often favored, particularly when used in combination with other forms of data for robust synchronization.

Synchronization using dynamic information follows a structured procedure: (i) the human motion during walking is analyzed to determine the relevant dynamic information, (ii) dynamic data, such as the thigh angle, is collected to estimate the gait phase, and (iii) based on the estimated gait phase, the prosthesis provides the appropriate trajectory at the exact moment. By relying on a gait phase estimation—rather than on absolute timing—this procedure enables synchronization independent of time. Specifically, the gait phase is derived by mapping a phase variable, generated from dynamic measurements that encompass user intent, to the gait cycle. As the gait progresses, the phase variable increases monotonically and linearly, ensuring a one-to-one correspondence to the gait cycle [18], [19], [20]. Such linearity and monotonicity guarantee that the gait progression can be reliably tracked without ambiguity or state transition errors.

This dynamic synchronization framework has been validated under various locomotion conditions, including level ground walking, slope walking, and stair walking. Focusing on level walking, several types of dynamic information have been harnessed to estimate the gait phase. For instance, Holgate et al. [21] utilized the tibia angle profile, though this method is only applicable to transtibial prostheses and is unsuitable for users of powered transfemoral prostheses. Another method employs the linearized hip position, which is also known to vary monotonically and linearly [22], [23], [24] although it requires additional sensing hardware attached to non-prosthetic body segments, potentially causing user discomfort.

A more commonly adopted strategy is to use the thigh angle, which follows a cosine-like waveform; by combining it with angular velocity or its integral, one obtains a phase variable that

Received 22 October 2024; accepted 30 May 2025. Date of publication 12 June 2025; date of current version 20 June 2025. This article was recommended for publication by Associate Editor M. Selvaggio and Editor K.-U. Kyung upon evaluation of the reviewers' comments. This work was supported in part by the Translational Research Program for Rehabilitation Robots under Grant #NRCTR-EX23002, #NRCTR-EX23003, and in part by the National Rehabilitation Center, Ministry of Health and Welfare, South Korea. *(Corresponding author: Pilwon Hur.)*

This work involved human subjects or animals in its research. Approval of all ethical and experimental procedures and protocols was granted by the Institutional Review Board (IRB) at Gwangju Institute of Science and Technology under Application No. 20230919-HR-73-02-02, and performed in line with the Declaration of Helsinki.

Myeongju Cha is with the Department of Mechanical and Robotics Engineering, Gwangju Institute of Science and Technology, Gwangju 61005, South Korea (e-mail: gistcmjgmj@gm.gist.ac.kr).

Pilwon Hur is with the Department of Mechanical and Robotics Engineering, Gwangju Institute of Science and Technology, Gwangju 61005, South Korea (e-mail: pilwonhur@gist.ac.kr).

Digital Object Identifier 10.1109/LRA.2025.3579634

increases monotonically and linearly [18], [19], [25], [26], [27], [28], [29], [30], [31], [32]. In transfemoral prostheses, thigh component can accommodate the necessary sensors, thereby eliminating the need for additional external equipment. By contrast, for transtibial users, an external sensor on the residual limb or the user's thigh segment may still be required. Even with this distinction, the thigh-based method remains advantageous because it addresses several limitations of the other two approaches, and has thus been widely adopted throughout the literature.

While extensive research has been conducted on phase estimation during level walking, there has been a noticeable lack of attention to phase estimation during stair walking, particularly stair descent. This research gap highlights the need for further investigation in this area. Although a few studies have focused on gait phase estimation during stair descent [33], and several others have examined stair ascent [3], [34], [35], the limited research on stair walking may hinder the development of lower limb powered prostheses that can provide natural movement during stair walking, unlike level walking. The scarcity of studies on gait phase estimation for stair descent likely arises from the challenge of identifying suitable candidates for phase variables. According to [20], the thigh angle does not follow a sinusoidal pattern during the stance phase of the gait cycle, making the phase estimation methods used for level walking unsuitable for stair descent. Therefore, a novel approach is needed to estimate the gait phase during stair descent.

In this letter, we propose a novel phase variable generation method for stair descent by utilizing more comprehensive information. The gait phase of stair descent is divided into two distinct phases: stance phase and swing phase. Phase variables are calculated separately for each phase using hip position and thigh angle, and these two variables are then unified into a single phase variable for the overall gait cycle of stair descent (see Section II). The results of this approach, including the phase variable calculations, are presented in Section IV, followed by a detailed discussion in Section V. The paper concludes with a summary of the key contributions and suggestions for future research directions in Section VI.

II. Methods

Our study utilized a phase variable-based estimation approach to determine the phase of stair descent walking. A gait cycle for stair descent walking is defined as a normalized period between two successive toe strikes, ranging from 0 to 1, with the toe striking the ground before the heel. The gait cycle consists of stance and swing phases, divided by the toe-off event, where the stance phase precedes toe-off and the swing phase follows it. After evaluating various options for phase variables, we identified hip position and thigh angle as the most influential parameters for formulating the phase variable during stair descent. Based on these two parameters, we developed distinct phase variables for the stance and swing phases: hip position was used during the stance phase, and thigh angle during the swing phase. To create a single, unified phase variable representing the entire gait cycle, we employed a blending method to ensure smooth transitions between the two phase variables. By combining the phase variables from each phase through this method, we formulated a comprehensive phase variable for the full stair descent gait cycle. Additionally, since certain variables cannot be measured until the end of the gait cycle, variables such as the range of the thigh angle and the integral of the thigh angle are estimated by averaging their values from previous gait cycles, ensuring feasibility for real-time implementation.

A. Phase Variable Candidates for Stair Descent

As mentioned in Section I, the thigh angle does not exhibit a sine-like pattern during the stance phase of stair descent walking, limiting its usefulness as a phase variable for the entire gait cycle. Therefore, additional information is needed to formulate a comprehensive phase variable. To be effective, a phase variable must be measurable by the prosthesis and reflect the wearer's intention, enabling precise control of a powered prosthetic leg. Based on these criteria, hip position and thigh angle were selected to formulate the phase variable for stair descent walking.

Hip position is defined as a horizontal (x) coordinate of the hip joint, which connects the pelvis and the thigh, relative to the toe position in the sagittal plane. Since the global position of the hip joint cannot be directly measured by sensors attached to the prosthesis during walking, the hip position is determined relative to the toe of the stance leg. It is calculated using the thigh, shank, and foot angles of the right lower limb in the sagittal plane. The thigh angle is defined as the angle between the vertical (y) axis and the thigh in the sagittal plane, with hip flexion considered the positive direction.

The hip position is used during the stance phase, while the thigh angle is used during the swing phase. As shown in Fig. 1, the hip position follows a linear and monotonic trend during the stance phase, making it suitable for formulating the phase variable for stair descent walking. Additionally, since the stance leg supports the entire body weight during this phase, the hip position reflects the wearer's intention to move forward. In contrast, during the swing phase, body weight is supported by the non-prosthetic leg, which lacks sensors to measure hip position. As a result, the hip position cannot be used as a phase variable during this phase, as it no longer reflects the wearer's intent to move forward. Instead, as shown in Fig. 1, the thigh angle during the swing phase follows a sine-like pattern, making it suitable for formulating the phase variable similarly to how it's done in level walking.

B. Phase Variable for the Stance Phase

During the stance phase of stair descent, the hip position shows a linear and monotonic trend in Fig. 1. Thus, a phase variable for the stance phase (PV-ST) can be generated by mapping the hip position to [0,1]. The hip position is measured throughout the stance phase (from 0% to toe-off timing of the gait) and mapped into [0,1] using the following equation.

$$\phi_{ST}(t) = \frac{x(t) - x(t_0)}{d_{avg}}, t_0 \leq t \leq t_{toe-off} \quad (1)$$

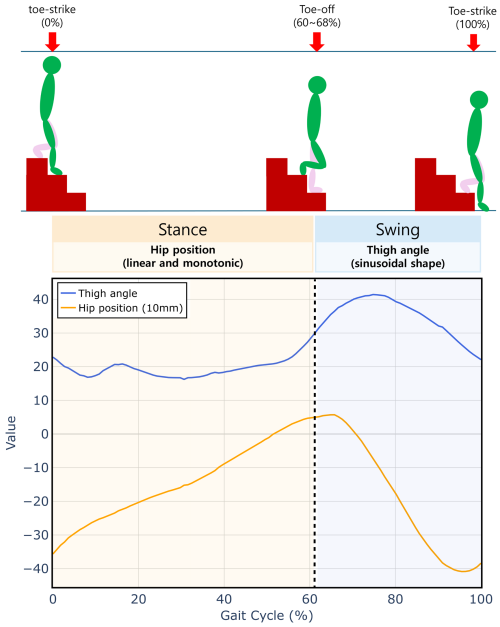

Fig. 1. Hip position and thigh angle trajectories during stair descent. The hip position shows a linear and monotonic trend during the stance phase, whereas the thigh angle shows a sinusoidal pattern during the swing phase. The dashed vertical line indicates the transition between stance and swing phases.

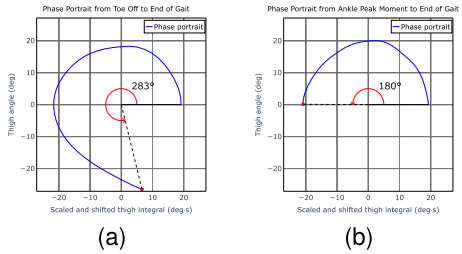

Fig. 2. Plot of phase portraits. (a) is a phase portrait with thigh angle and integral of thigh angle from toe-off to the end of the gait. (b) is a phase portrait with thigh angle and integral of thigh angle from ankle peak moment to the end of the gait. (a) does not show a semicircular shape, but (b) shows a semicircular shape. The angle measured from these phase portraits is used to generate the phase variable.

where, $\phi_{ST}(t)$ is the phase variable during the stance phase (PV-ST), $x(t)$ is hip position at time t, t_0 is the time corresponding to 0% of the gait cycle, and $t_{toe-off}$ is the time when toe-off occurs, and d_{avg} is the average displacement from $x(t_0)$ to $x(t_{toe-off})$ over all previous steps.

C. Phase Variable for the Swing Phase

During the swing phase, the thigh angle exhibits a sinusoidal trajectory. When this thigh angle is plotted against its integral (appropriately scaled and shifted) a phase portrait is formed, characteristically displaying a clear semicircular shape, as illustrated in Fig. 2(a). Leveraging this semicircular phase portrait, the gait phase can be effectively determined by measuring the angle formed between the horizontal axis and the line connecting each point on the portrait to the origin. This measured angle spans from 0 to 4.94 radians (283 degrees) and is subsequently mapped onto a normalized gait phase range from 0 (0%) to 1 (100%), thereby providing a monotonic and continuous representation of gait progression.

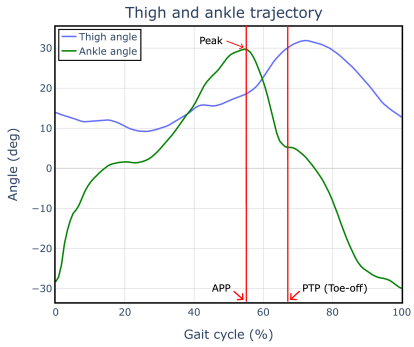

Fig. 3. Plot of thigh and ankle angles. Red lines represent gait events defined in this study. Ankle peak point (APP) is the point at which the ankle angle reaches its peak. Phase transition point (PTP) is the point at which the phase transition happens. The PTP happens at toe-off which distinguishes the stance and swing phase. In this plot, the thigh angle follows the shape of a half-period of a sine wave when investigating the range from APP to PTP.

However, a challenge arises in generating a reliable phase variable during the swing phase. When the phase portrait is initiated from the beginning of the swing phase (phase transition point in gait cycle, PTP), the initial and final thigh angle values differ significantly, causing the phase portrait to deviate from a clear half-periodic pattern (Fig. 2(a)). Consequently, the angle measured from this phase portrait at the end of the gait cycle lacks consistency, complicating the accurate mapping of this angle onto the normalized gait phase range [0,1]. To address this issue, the initiation point for generating the phase portrait is adjusted to a moment at which the thigh angle exhibits a consistent, half-periodic behavior. Specifically, the integration of the thigh angle is initiated from the ankle angle peak point (ankle peak point in gait cycle, APP), identified just prior to the swing phase onset. As depicted in Fig. 3, from this ankle peak point until the end of the swing phase, the thigh angle closely approximates a half-periodic sinusoidal trajectory. By selecting this optimized initiation point, the resulting phase portrait reliably forms a semicircular pattern, enabling the measurement of a consistent angle that can be precisely and monotonically mapped onto the gait phase range from 0 to 1. Moreover, since the average location of PTP within the gait cycle can be calculated from the past gait data, the phase variable calculated from APP to the end of the gait can be easily remapped to represent the swing phase (PTP to end of the gait).

After determining the optimal integration starting point (ankle peak moment, APP), the swing phase variable (PV-SW) can be defined using the following equation:

$$\phi_{SW}(t) = \frac{\phi_{SW}^{temp}(t) - \phi_{SW}^{temp}(t_{PTP})}{1 - \phi_{SW}^{temp}(t_{PTP})} \tag{2}$$

Here, $\phi_{SW}^{temp}(t)$ is a temporary phase variable calculated from the ankle peak moment (APP) to the end of the gait cycle. To adjust this temporary phase variable to align precisely with the swing phase (from PTP to gait end), we normalize it by subtracting its value at the swing phase initiation time, t_{PTP}, and scaling it accordingly. The temporary phase variable is expressed

mathematically as follows:

$$\phi_{SW}^{temp}(t)=\frac{1}{\pi}\,\mathrm{atan2}((\theta_{TH}(t)-\theta_{TH}(t_{APP}),k(\Theta_{TH}(t)-\alpha)) \tag{3}$$

$$\Theta_{TH}(t)=\int_{t_{APP}}^{t}(\theta_{TH}(\tau)-\theta_{TH}(t_{APP}))\,d\tau \tag{4}$$

$$\alpha=\frac{(\Theta_{TH}^{max}+\Theta_{TH}^{min})}{2},k=-\frac{|\theta_{TH}^{max}-\theta_{TH}(t_{APP})|}{|\Theta_{TH}^{max}-\Theta_{TH}^{min}|} \tag{5}$$

where $\theta_{TH}(t)$ denotes the thigh angle at time t, t_{APP} is the ankle peak moment, and t_{PTP} is swing phase initiation (phase transition point, PTP). Additionally, $\Theta_{TH}(t)$ represents the integral of the thigh angle, adjusted by subtracting its initial value at t_{APP} while parameters α and k shift and scale this integral to produce a semicircular trajectory in the phase portrait. The maximum and minimum values of the thigh angle and its integral cannot be directly obtained within the same gait cycle in real-time implementation. Thus, these values are practically estimated using averages derived from previous gait cycles, enabling continuous, real-time gait phase estimation.

By initiating integration at the ankle peak moment, the resulting temporary phase variable consistently approaches 1 at the end of the gait cycle, providing a robust and monotonic measure of gait progression. However, as the temporary variable begins slightly before the actual swing phase, the portion preceding the swing phase (prior to t_{PTP}) is excluded. Consequently, the remaining segment—from swing phase initiation (PTP) to gait end—is rescaled onto a normalized range [0,1], accurately representing the swing phase progression.

Note the events APP and PTP are represented as percentages of the gait cycle for clarity (Fig. 3). In mathematical formulations above, however, these events correspond to specific moments in time, denoted as t_{APP} and t_{PTP}, respectively.

D. Phase Variable for the Entire Gait Cycle

Finally, the phase variables generated during the stance and swing phases are combined into a single phase variable. To achieve this, a normalized ratio corresponding to the phase transition point (r_{PTP}) must be accurately identified to map the phase variables across the entire gait cycle. Calculating the precise r_{PTP} requires knowing the ratio of the total gait time to the time elapsed from the beginning of the gait cycle to the toe-off event, which can only be determined after the cycle is complete. Therefore, the average r_{PTP} from previous gait cycles is used as the r_{PTP} for the current gait, allowing for real-time application of the phase variable.

After determining the r_{PTP}, the phase variable for the entire gait cycle can be calculated using the following equation.

$$\phi(t)=\begin{cases}r_{PTP}\times\phi_{ST}(t), & t_{init}\le t\le t_{PTP}\\ \phi_1+(1-r_{PTP})\times\phi_{SW}(t), & t_{PTP}<t\le t_{fin}\end{cases} \tag{6}$$

where $\phi(t)$ is the unified phase variable for the entire gait cycle (PV-ENT), $\phi_{ST}(t)$ is the phase variable for the stance phase (PV-ST), $\phi_{SW}(t)$ is the phase variable for the swing phase (PV-SW), ϕ_1 equals to $\phi(t_{PTP})$, t_{init} is the initial time of the gait, and t_{fin} is the time when the gait ends.

E. Blending Method

Despite the formulation of the unified phase variable $\phi(t)$ for the entire gait cycle (PV-ENT), there remains an issue. When PV-ENT is calculated using (6), a non-smooth transition occurs at the phase transition point (PTP). Given that the prosthesis generates motion based on this phase variable, such non-smooth transitions may induce abrupt prosthetic movements, potentially resulting in discomfort for the user. This non-smoothness arises primarily because the unified phase variable defined by (6) directly concatenates two independently normalized variables, $\phi_{ST}(t)$ and $\phi_{SW}(t)$, at PTP, without without adequately ensuring continuity in their values and derivatives.

To address this challenge and achieve a smoother transition, we introduce a blending method. This method calculates a weighted average of two phase variables (stance phase variable and temporary swing phase variable) over the region spanning from the ankle peak point APP to the phase transition point (PTP). The temporary swing phase variable is employed rather than the finalized swing phase variable defined in (2), as the latter does not encompass the interval between APP and PTP. This blending approach ensures smooth and continuous transitions between the stance and swing phase variables. The detailed implementation of this blending method is described by the following equations:

$$\phi(t)=\begin{cases}r_{PTP}\times\phi_{ST}(t), & t_{init}\le t\le t_{APP}\\ \phi_2+\phi_B(t), & t_{APP}<t\le t_B\\ \phi_3+\phi_{SW}^{\triangle}(t), & t_B<t\le t_{fin}\end{cases} \tag{7}$$

where,

$$\phi_2=\phi(t_{APP}),\phi_3=\phi(t_B), \tag{8}$$

$$\phi_{SW}^{\triangle}(t)=\frac{(1-\phi_3)}{1-\phi_{SW}^{temp}(t_B)}(\phi_{SW}^{temp}(t)-\phi_{SW}^{temp}(t_B)), \tag{9}$$

$$\phi_B(t)=\omega(t)\phi_{ST}^{B}(t)+(1-\omega(t))\phi_{SW}^{B}(t), \tag{10}$$

t_B is the time when the blending is completed, and $\phi_B(t)$ is the blended phase variable, defined as a weighted average of phase variables from the stance and swing phase.

In (7), the blending method is applied over the range from t_{APP} to t_B using $\phi_B(t)$. To define $\phi_B(t)$, the following additional information is needed.

$$\omega(t)=\frac{T-\phi(t-\Delta t)}{T-\phi(t_{APP})}, \tag{11}$$

$$\phi_{ST}^{B}(t)=r_{PTP}\times(\phi_{ST}(t)-\phi_{ST}(t_{APP})), \tag{12}$$

$$\phi_{SW}^{B}(t)=(1-r_{APP})\times\phi_{SW}^{temp}(t), \tag{13}$$

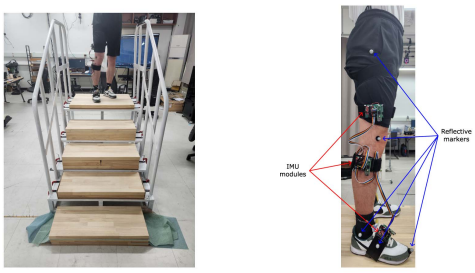

Fig. 4. Experimental device setup. (a) Staircase with four steps, each measuring 185 mm in height, 300 mm in length, and 1 m in width. (b) Reflective markers and IMU modules attached to the right lower limb. Reflective markers are placed on the hip, knee, and ankle joints, side of the foot, and toe, while IMU modules are placed on thigh, shank, and foot.

where Δt is the sampling time, T is the threshold for stopping the blending, and r_{APP} represents the normalized ratio corresponding to the ankle peak point (APP). It should be noted that in the calculation of $\omega(t)$, since the value of the phase variable at time t is unknown prior to computation, the phase variable from the previous time step $(t - \Delta t)$ is used. In addition, if $\phi(t)$ reaches T at time $\hat{t}$, the blending is terminated and $\hat{t}$ becomes t_B. T is determined as follows.

$$T = (1 - \omega_T) r_{APP} + \omega_T r_{PTP} \tag{14}$$

where ω_T is the weight for calculating T. In this letter, ω_T is set to 0.2, ensuring that the computed phase variables remain smooth throughout the blending region based on experimental validation. Furthermore, consistent with the reasoning presented in Section II-D, r_{APP} and r_{PTP} values for the current gait cycle are determined from the average values of previous gait cycles, guaranteeing real-time applicability.

Moreover, the phase variables from each phase are normalized to estimate the phase from the ankle peak point to the phase transition point, as described in the equations for $\phi^B_{ST}(t)$ and $\phi^B_{SW}(t)$. By normalizing them, the weighted average can be calculated as (10). Specifically, $\phi_{ST}(t)$ is shifted such that $\phi_{ST}(t)$ equals zero at the starting point of the blending region. If $\phi_{ST}(t)$ is not adjusted to zero at that point, $\phi_B(t)$ would consequently deviate from zero, potentially causing a discontinuous transition at t_{APP}.

III. Experiment

A. Experimental Setup

A stair descent experiment was conducted to validate the proposed phase variable (Fig. 4). The staircase, consisting of four steps with a height of 185 mm, a length of 300 mm, and a width of 1 m, was positioned under nine motion capture cameras (NOKOV, 100 Hz). Reflective markers and IMU modules (MPU9250, 100 Hz) were attached to subjects. The marker and IMU data were used to separately obtain the positions of the thigh, knee, ankle, and hip. Additionally, toe-strike and toe-off timings were detected using the motion capture data.

B. Experimental Protocol

Twelve healthy young subjects (5 females, 7 males; age: 24.42 ± 3.06 years, height: 168.78 ± 9.64 cm, weight: 62.75 ± 9.93 kg) participated in the experiment with markers attached to their bodies. Subjects performed three test walks to adjust the marker positions for optimal recognition during stair descent. After adjusting the markers, a 5-minute training session was conducted to collect data under natural stair descent conditions. If the subject felt comfortable with the walking, the training session was concluded before the 5 minutes elapsed. Following the test and training sessions, the experiment proceeded as described below.

1) The subject stood atop of the stairs with comfort.
2) After the start signal, the subject began walking down the stairs, stepping first with the right foot.
3) When the subject stepped onto the ground with the right foot, they finished walking and placed both feet at the same horizontal position in the sagittal plane.
4) Steps 1-3 were repeated 20 times.

During the experiment, 0.9 m handrails were attached to both the left and right sides of the stairs to ensure the safety of the subjects. The experimental protocol was approved by the Institutional Review Board (IRB) at the Gwangju Institute of Science and Technology (20230919–HR–73–02–02).

C. Data Processing and Statistical Analysis

After the experiment, marker data were saved as C3D files using the motion capture program (NOKOV), and IMU data were saved as CSV files. The motion capture system was used to establish ground truth data and validate the ideal phase estimation based on this ground truth. Since motion capture cannot be used for real-time prosthesis control but IMU data can, the IMU data were collected to assess whether the proposed phase variable could be applied for prosthesis control. Of the 20 trials, several data sets were excluded from processing. The first two were excluded due to subject familiarization with the stairs, and the 19th and 20th were excluded to mitigate the effects of fatigue. Trials with missing marker data were also excluded, leaving 10 valid trials per subject for processing. Using Julia (version 1.10.4), joint information (thigh and ankle angles, hip position) and gait event timing (toe-off and toe-strike) were calculated. The phase variable was then computed based on this data using the proposed phase generation method.

To evaluate performance and the effect of the blending method, R^2 and Root Mean Square Error (RMSE) were used to assess linearity, while the maximum absolute value of the second derivative of the phase variable, $S_{\max}$, was used to evaluate smoothness. R^2 and RMSE measure how closely the phase variable follows a linear function, with $R^2 = 1.0$ and RMSE $=$ 0.0 indicating a perfect match. $S_{\max}$ was used to assess smoothness at the transition between the stance and swing phases, where non-smoothness typically occurs. Specifically, $S_{\max}$ was analyzed in the range from 40% to 80% of the gait cycle, where the blending is applied. This range was chosen because the average APP is approximately 0.5, and the average PTP lies

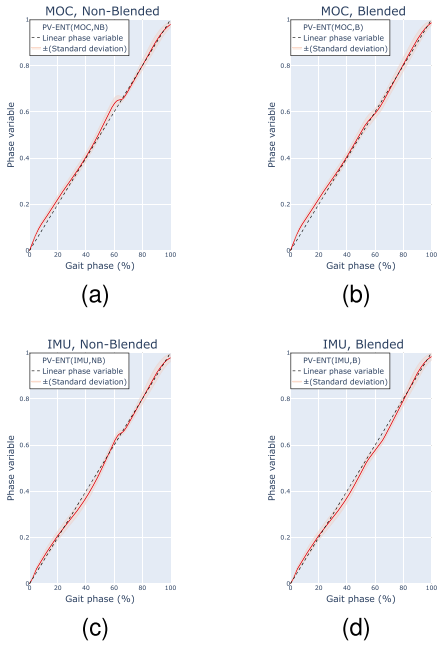

Fig. 5. Plot of the phase variable calculated by the experimental data from motion capture system and IMU sensors. In the title of each figure, MOC means that the motion capture data is used, IMU means that the IMU data is used. In addition, the blended means that the blending method is applied and non-blended means that the blending method is not applied. For all plots, the black dashed line is linear function. If the phase variable is linear function, then, the estimated gait phase equals the real gait phase. The pink shade area indicates the standard deviation.

between 0.6 and 0.7 (see Fig. 3). A two-way repeated-measures ANOVA was performed to assess the statistical significance of the effects of data source and the blending method on these metrics (RStudio, Boston, MA, USA). The level of significance was set to $\alpha = 0.05$.

D. Real-Time Validation Experiment

Additional real-time validation experiments were conducted with three non-disabled subjects (one female, two males; age: 24.33 ± 0.47 years, height: 169.67 ± 2.87 cm, weight: 73.00 ± 13.64 kg) to assess the feasibility of real-time implementation. Subjects wore IMU sensors and force-sensitive resistors (FSRs), with sensor data processed in real-time (100 Hz) using a portable computing unit (Jetson Nano) carried by subjects in a backpack. Subjects performed stair descent walking on a staircase consisting of 12 steps (height: 158 mm, length: 300 mm), and the phase variable was calculated in real-time on the portable device. The subject walked down the stairs for 20 trials. Performance metrics (R^2, RMSE, $S_{\max}$) were computed just as the offline evaluations described previously.

IV. Results

The proposed method was applied to the experimental data, and the resulting phase variables are shown in Fig. 5. The figure compares the phase variables for stair descent under two conditions: i) motion capture data vs. IMU data and ii) blending vs. no blending. This comparison illustrates the effects of using different data sources (i.e., sensors) and the impact of applying the blending method on the phase variable. In the following subsections, the performance of the proposed phase variables for the stair descent will be analyzed based on the linearity and smoothness.

TABLE I
Comparison of R^2 Values and RMSE for Phase Variables With and Without Blending for Motion Capture and IMU Data.

Data Source	Blend	R^2 Value	RMSE
Motion Capture	Yes	0.9920 ± 0.0045	0.0246 ± 0.0083
	No	0.9922 ± 0.0049	0.0241 ± 0.0087
IMU	Yes	0.9911 ± 0.0073	0.0255 ± 0.0101
	No	0.9926 ± 0.0067	0.0227 ± 0.0104

Note that no statistical significance was found in any of the comparisons.

TABLE II
Comparison of Smoothness ($S_{\max}$ of Phase Variables Generated by Proposed Method)

Blending	Data Source	S_{max} value	p-value
Yes	Motion Capture	16.6070 ± 4.7227	< 0.001
	IMU	17.3143 ± 4.0714	
No	Motion Capture	39.4476 ± 13.2436	
	IMU	38.4451 ± 12.4865	

A. Linearity

The linearity of the phase variables generated using the proposed method was evaluated by comparing the R^2 values and RMS error values from motion capture and IMU data, with and without the use of blending. As shown in Table I, the phase variables generated from both motion capture and IMU data sources demonstrate high linearity in terms of R^2 values, regardless of whether blending was applied. For the motion capture data, the R^2 values were 0.9920 ± 0.0045 and 0.9922 ± 0.0049 with and without blending, respectively. Similarly, for the IMU data, the R^2 values were 0.9911 ± 0.0073 and 0.9926 ± 0.0067 with and without blending, respectively. There were no main effects of data source (i.e., motion capture vs. IMU, $p = 0.670$) and blending methods (i.e., with and without blending, $p = 0.885$) on R^2 values.

Regarding RMSE, the results show a similar level of linearity. For the motion capture data, the RMS error was 0.0246 ± 0.0083 with blending and 0.0241 ± 0.0087 without blending. For the IMU data, the RMSE with blending was 0.0255 ± 0.0101, while without blending, it was 0.0227 ± 0.0104. There were no main effects of data source (i.e., motion capture vs. IMU, $p = 0.571$) and blending methods (i.e., with and without blending, $p = 0.813$) on RMSE.

B. Smoothness

The smoothness of the phase variables generated using the proposed method was evaluated by comparing the $S_{\max}$ values from motion capture and IMU data, with and without the use of blending. In Table II, the smoothness significantly improved for phase variables from both motion capture and IMU data after applying the blending method ($p < 0.001$). Specifically, $S_{\max}$ decreased by 57.90% (from 39.4476 to 16.6070) for the motion capture data and by 54.96% (from 38.4451 to 17.3143) for the IMU data.

TABLE III
REAL-TIME VALIDATION RESULTS FOR EACH SUBJECT

Sub	Blend	RMSE	R^2 value	S_{max} value
1	No	0.0595 ± 0.0189	0.9605 ± 0.0247	258.329 ± 116.121
	Yes	0.0542 ± 0.0117	0.9685 ± 0.0131	263.842 ± 169.122
2	No	0.0490 ± 0.0188	0.9709 ± 0.0217	120.3730 ± 64.354
	Yes	0.0406 ± 0.0103	0.9784 ± 0.0114	251.578 ± 166.671
3	No	0.0619 ± 0.0139	0.9644 ± 0.0141	153.463 ± 77.572
	Yes	0.0446 ± 0.0098	0.9801 ± 0.0082	197.979 ± 81.817

C. Real-Time Validation Results

The real-time validation experiments indicated slightly reduced performance relative to the offline evaluations. For the blended phase variable, the mean RMSE was 0.0462 ± 0.0118, and the mean R^2 was 0.9763 ± 0.0118. These results represent slight improvements compared to the non-blended phase variable (RMSE: 0.0574 ± 0.0177, R^2: 0.9652 ± 0.0201). However, the smoothness quantified by $S_{\max}$ slightly deteriorated after applying the blending method, increasing from 174.57 ± 103.33 to 233.11 ± 141.10. Detailed performance metrics for individual subjects are presented in Table III.

V. DISCUSSION

Using the method proposed in this letter, the phase variable (PV-ENT) for stair descent gait was generated. Given the scarcity of studies explicitly addressing stair descent, direct comparisons were limited. Hence, we compared our approach with well-established methods for level-ground walking, reasoning that achieving similar or superior performance (RMSE, R^2) in the more challenging stair-descent scenario validates our method. PV-ENT demonstrated superior accuracy and linearity (RMSE $= 0.0255$, $R^2 = 0.9911$) compared to PS-PV2 (RMSE $= 0.0367$, $R^2 = 0.9886$) from Hong et al. [25], who proposed a thigh angle-based phase variable using phase portraits for level walking. Additionally, our method outperformed the neural network-based phase estimator by Kang et al. [36], which utilized thigh angles and hip torques to control a hip exoskeleton (RMSE $= 0.0910$ for stair descent, 0.0363 for stair ascent). These comparisons, summarized visually in Fig. 6, further confirm the reliability and accuracy of PV-ENT.

Although adaptive oscillator-based algorithms have demonstrated robust synchronization capabilities in periodic gait scenarios, explicit validation in more variable conditions such as stair descent remains limited. Consequently, our PV-ENT method was primarily compared with methods utilizing similar sensor inputs and phase variable generation methods (e.g., thigh angle and phase portraits [25]), providing a specialized and validated approach for stair descent gait. Future studies directly comparing adaptive oscillator-based methods under similar conditions would help further clarify their relative strengths and limitations.

The blending algorithm effectively resolved potential jerkiness at stance-to-swing transitions, significantly enhancing smoothness ($S_{\max}$) without statistically impacting accuracy and linearity (RMSE and R^2). The real-time validation demonstrated slightly reduced accuracy (mean RMSE $= 0.0462$, mean $R^2 = 0.9763$) compared to offline evaluations, likely due to sensor noise and latency in gait-event detection from real-time use of force-sensitive resistors. These delays impacted smoothness during blending. Nonetheless, the recursive real-time estimation results (Fig. 7) confirmed that our algorithm can adapt and synchronize the estimated phase variable with actual gait progression across consecutive cycles, highlighting practical reliability and underscoring the need for further optimization in sensor integration and gait event detection methods.

Several limitations of our approach exist. First, while transfemoral prostheses naturally accommodate sensors, transtibial prostheses require external sensors attached to the user's thigh, potentially causing inconvenience. Additionally, the current real-time validation was conducted without an active powered prosthesis, so further validation using actual prosthetic hardware is needed. For transfemoral prostheses, sensor integration issues may be mitigated by utilizing knee and ankle motor encoders. Lastly, this study focused solely on stair descent, and future work should include higher-level gait mode detection systems to facilitate seamless locomotion mode transitions.

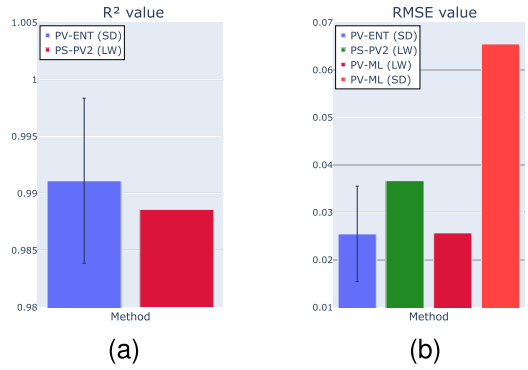

Fig. 6. Bar plots of R^2 (a) and RMSE (b) of the phase variables from this study and the compared studies. PV-ENT is the phase variable calculated in this study from the IMU data with the blending method. PS-PV2 is the phase variable from [25]. PV-ML is from [36]. SD means that the phase variable is for stair descent, and LW means that the phase variable is for level walking.

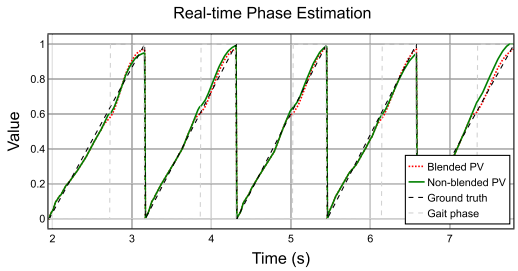

Fig. 7. Representative example of real-time recursive estimation of the phase variable across consecutive stair descent gait cycles. The dashed black line represents the ground truth phase variable derived from motion capture data, the solid green line indicates the real-time estimated non-blended phase variable, and the dotted red line shows the real-time estimated blended phase variable. Vertical gray dashed lines indicate the gait phase (swing or stance phase) of the gait cycle. 0 and 1 correspond to the stance and swing phase. This example illustrates how the proposed phase estimation algorithm recursively adapts and maintains synchronization with the actual gait progression in real-time conditions.

VI. Conclusion

In this study, we proposed a novel phase variable-based gait phase estimation method for stair descent using hip position and thigh angle data. Unlike previous studies primarily focused on level-ground walking, this approach addressed the specific challenges associated with stair descent. Separate phase variables for stance and swing phases were unified into a single phase variable for the entire gait cycle, and a blending method was introduced to ensure smooth transitions at the stance-to-swing boundary without compromising accuracy. Offline comparisons with related studies demonstrated the reliability of the proposed method, while real-time validation experiments confirmed its practical applicability, achieving reliable linearity (mean $R^2 = 0.9763$) and accuracy (mean RMSE $= 0.0462$). Although slight reductions in smoothness were observed under real-time conditions, the blending approach provided clear advantages over the non-blended method. Future work will focus on validating the method through real-time implementation with powered prostheses, integrating higher-level gait mode detection systems for seamless transitions across different locomotion scenarios, and further optimizing computational efficiency and gait-event detection accuracy to enhance robustness in practical prosthetic applications.

References

[1] S. K. Au, J. Weber, and H. Herr, "Powered ankle–foot prosthesis improves walking metabolic economy," *IEEE Trans. Robot.*, vol. 25, no. 1, pp. 51–66, Feb. 2009.

[2] H. M. Herr and A. M. Grabowski, "Bionic ankle–foot prosthesis normalizes walking gait for persons with leg amputation," *Proc. Roy. Soc. B, Biol. Sci.*, vol. 279, no. 1728, pp. 457–464, 2012.

[3] E. Ledoux and M. Goldfarb, "Control and evaluation of a powered transfemoral prosthesis for stair ascent," *IEEE Trans. Neural Syst. Rehabil. Eng.*, vol. 25, no. 7, pp. 917–924, Jul. 2017.

[4] E. C. Martinez-Villalpando, L. Mooney, G. Elliott, and H. Herr, "Antagonistic active knee prosthesis. a metabolic cost of walking comparison with a variable-damping prosthetic knee," in *Proc. Annu. Int. Conf. IEEE Eng. Med. Biol. Soc.*, IEEE, 2011, pp. 8519–8522.

[5] W. Hong et al., "Empirical validation of an auxetic structured foot with the powered transfemoral prosthesis," *IEEE RA-L*, vol. 7, no. 4, pp. 11228–11235, Oct. 2022.

[6] W. Hong, J. Lee, and P. Hur, "Effect of torso kinematics on gait phase estimation for enhancing speed adaptability," *Front. Neurorobot.*, vol. 16, 2022, Art. no. 807826.

[7] S. Patrick, N. Anil Kumar, W. Hong, and P. Hur, "Biomechanical impacts of toe joint with transfemoral amputee using a powered knee-ankle prosthesis," *Front. Neurorobot.*, vol. 16, 2022, Art. no. 809380.

[8] N. Anil Kumar, S. Patrick, W. Hong, and P. Hur, "Control framework for sloped walking with a powered transfemoral prosthesis," *Front. Neurorobot.*, vol. 15, 2022, Art. no. 790060.

[9] S. Huang, J. Wensman, and D. Ferris, "An experimental powered lower limb prosthesis using proportional myoelectric control," *J. Med. Devices*, vol. 8, no. 2, 2014, Art. no. 024501.

[10] H. Huang, T. A. Kuiken, and R. D. Lipschutz, "A strategy for identifying locomotion modes using surface electromyography," *IEEE Trans. Biomed. Eng.*, vol. 56, no. 1, pp. 65–73, Jan. 2009.

[11] S. Huang, J. Wensman, and D. Ferris, "Locomotor adaptation by transtibial amputees walking with an experimental powered prosthesis under continuous myoelectric control," *IEEE Trans. Neural Syst. Rehabil. Eng.*, vol. 24, no. 5, pp. 573–581, May 2016.

[12] G. Horn, "Electro-control: AM EMG-controlled A/K prosthesis," *Med. Biol. Eng.*, vol. 10, pp. 61–73, 1972.

[13] H. Huang, F. Zhang, L. J. Hargrove, Z. Dou, D. R. Rogers, and K. B. Englehart, "Continuous locomotion-mode identification for prosthetic legs based on neuromuscular–mechanical fusion," *IEEE Trans. Biomed. Eng.*, vol. 58, no. 10, pp. 2867–2875, Oct. 2011.

[14] J. A. Dawley, K. B. Fite, and G. D. Fulk, "EMG control of a bionic knee prosthesis: Exploiting muscle co-contractions for improved locomotor function," in *Proc. IEEE 13th Int. Conf. Rehabil. Robot.*, IEEE, 2013, pp. 1–6.

[15] J. Wang, O. A. Kannape, and H. M. Herr, "Proportional EMG control of ankle plantar flexion in a powered transtibial prosthesis," in *Proc. IEEE 13th Int. Conf. Rehabil. Robot.*, IEEE, 2013, pp. 1–5.

[16] L. J. Hargrove et al., "Robotic leg control with EMG decoding in an amputee with nerve transfers," *New England J. Med.*, vol. 369, no. 13, pp. 1237–1242, 2013.

[17] M. Tschiedel, M. F. Russold, and E. Kaniusas, "Relying on more sense for enhancing lower limb prostheses control: A review," *J. Neuroeng. Rehabil.*, vol. 17, pp. 1–13, 2020.

[18] D. Quintero, D. J. Villarreal, D. J. Lambert, S. Kapp, and R. D. Gregg, "Continuous-phase control of a powered knee–ankle prosthesis: Amputee experiments across speeds and inclines," *IEEE Trans. Robot.*, vol. 34, no. 3, pp. 686–701, Jun. 2018.

[19] D. J. Villarreal, H. A. Poonawala, and R. D. Gregg, "A robust parameterization of human gait patterns across phase-shifting perturbations," *IEEE Trans. Neural Syst. Rehabil. Eng.*, vol. 25, no. 3, pp. 265–278, Mar. 2017.

[20] D. J. Villarreal and R. D. Gregg, "A survey of phase variable candidates of human locomotion," in *Proc. 36th Annu. Int. Conf. IEEE Eng. Med. Biol. Soc.*, IEEE, 2014, pp. 4017–4021.

[21] M. A. Holgate, T. G. Sugar, and A. W. Bohler, "A novel control algorithm for wearable robotics using phase plane invariants," in *Proc. IEEE Int. Conf. Robot. Autom.*, IEEE, 2009, pp. 3845–3850.

[22] V. Paredes, W. Hong, S. Patrick, and P. Hur, "Upslope walking with transfemoral prosthesis using optimization based spline generation," in *Proc. IEEE/RSJ Int. Conf. Intell. Robots Syst.*, 2016, pp. 3204–3211.

[23] H. Zhao, J. Horn, J. Reher, V. Paredes, and A. D. Ames, "First steps toward translating robotic walking to prostheses: A nonlinear optimization based control approach," *Auton. Robots*, vol. 41, pp. 725–742, 2017.

[24] H. Zhao, J. Reher, J. Horn, V. Paredes, and A. D. Ames, "Realization of nonlinear real-time optimization based controllers on self-contained transfemoral prosthesis," in *Proc. ACM/IEEE 6th Int. Conf. Cyber- Phys. Syst.*, 2015, pp. 130–138.

[25] W. Hong, N. A. Kumar, and P. Hur, "A phase-shifting based human gait phase estimation for powered transfemoral prostheses," *IEEE Robot. Autom. Lett.*, vol. 6, no. 3, pp. 5113–5120, Jul. 2021.

[26] D. J. Villarreal and R. D. Gregg, "Controlling a powered transfemoral prosthetic leg using a unified phase variable," in *Wearable Robotics*. Amsterdam, The Netherlands: Elsevier, 2020, pp. 487–506.

[27] A. Naeem et al., "Virtual constraint control of knee-ankle prosthesis using an improved estimate of the thigh phase-variable," *Biomed. Signal Process. Control*, vol. 73, 2022, Art. no. 103366.

[28] T. Ma et al., "A piecewise monotonic smooth phase variable for speed-adaptation control of powered knee-ankle prostheses," *IEEE Robot. Autom. Lett.*, vol. 7, no. 3, pp. 8526–8533, Jul. 2022.

[29] W. Hong, N. A. Kumar, S. Patrick, S. Moon, and P. Hur, "A feasibility study of piecewise phase variable based on variable toe-off for the powered prosthesis control: A case study," *IEEE Robot. Autom. Lett.*, vol. 8, no. 5, pp. 2590–2597, May 2023.

[30] D. J. Villarreal and R. D. Gregg, "Unified phase variables of relative degree two for human locomotion," in *Proc. 38th Annu. Int. Conf. IEEE Eng. Med. Biol. Soc.*, IEEE, 2016, pp. 6262–6267.

[31] W. Hong, J. Lee, and P. Hur, "Piecewise linear labeling method for speed-adaptability enhancement in human gait phase estimation," *IEEE Trans. Neural Syst. Rehabil. Eng.*, vol. 31, pp. 628–635, 2023.

[32] J. Lee, W. Hong, and P. Hur, "Continuous gait phase estimation using LSTM for robotic transfemoral prosthesis across walking speeds," *IEEE Trans. Neural Syst. Rehabil. Eng.*, vol. 29, pp. 1470–1477, 2021.

[33] R. J. Cortino, T. K. Best, and R. D. Gregg, "Data-driven phase-based control of a powered knee-ankle prosthesis for variable-incline stair ascent and descent," *IEEE Trans. Med. Robot. Bionics*, vol. 6, no. 1, pp. 175–188, Feb. 2024.

[34] S. Hood, L. Gabert, and T. Lenzi, "Powered knee and ankle prosthesis with adaptive control enables climbing stairs with different stair heights, cadences, and gait patterns," *IEEE Trans. Robot.*, vol. 38, no. 3, pp. 1430–1441, Jun. 2022.

[35] R. J. Cortino, E. Bolívar-Nieto, T. K. Best, and R. D. Gregg, "Stair ascent phase-variable control of a powered knee-ankle prosthesis," in *Proc. Int. Conf. Robot. Autom.*, IEEE, 2022, pp. 5673–5678.

[36] I. Kang, D. D. Molinaro, S. Duggal, Y. Chen, P. Kunapuli, and A. J. Young, "Real-time gait phase estimation for robotic hip exoskeleton control during multimodal locomotion," *IEEE Robot. Autom. Lett.*, vol. 6, no. 2, pp. 3491–3497, Apr. 2021.